

1
2
3 1 TITLE: The sensitivity of US wildfire occurrence to pre-season soil moisture conditions
4 2 across ecosystems
5
6 3

7 4 AUTHORS: Daniel Jensen¹, John T. Reager^{2*}, Brittany Zajic¹, Nick Rousseau¹, Matthew Rodell³,
8 5 and Everett Hinkley⁴

9
10 6
11 7 ¹NASA DEVELOP National Program, Science Systems and Applications, Inc.
12
13 8 NASA Jet Propulsion Laboratory, California Institute of Technology, Pasadena, California, USA
14
15 9 ³NASA Goddard Space Flight Center, Greenbelt, Maryland, USA
16
17 10 ⁴National Remote Sensing Program Manager, USDA Forest Service, 1400 Independence Ave.,
18 SW, Washington, DC 20250, USA
19
20
21 13 *Correspondence to:
22 14 John T. Reager
23 15 Email: John.Reager@jpl.nasa.gov
24
25
26
27
28
29
30
31
32
33
34
35
36
37
38
39
40
41
42
43
44
45
46
47
48
49
50
51
52
53
54
55
56
57
58
59
60

1
2
3 41 ABSTRACT
4
5
6

7
8
9
10
11
12
13
14
15
16
17
18
19
20
21
22
23
24
25
26
27
28
29
30
31
32
33
34
35
36
37
38
39
40
41
42
43
44
45
46
47
48
49
50
51
52
53
54
55
56
57
58
59
60

It is generally accepted that year-to-year variability in moisture conditions and drought are linked with increased wildfire occurrence. However, quantifying the sensitivity of wildfire to surface moisture state at seasonal lead-times has been challenging due to the absence of a long soil moisture record with the appropriate coverage and spatial resolution for continental-scale analysis. Here we apply model simulations of surface soil moisture that numerically assimilate observations from NASA's Gravity Recovery and Climate Experiment (GRACE) mission with the US Forest Service's historical Fire-Occurrence Database over the contiguous United States. We quantify the relationships between pre-fire-season soil moisture and subsequent-year wildfire occurrence by land-cover type and produce annual probable wildfire occurrence and burned area maps at 0.25-degree resolution. Cross-validated results generally indicate a higher occurrence of smaller fires when months preceding fire season are wet, while larger fires are more frequent when soils are dry. This result is consistent with the concept of increased fuel accumulation under wet conditions in the pre-season. These results demonstrate the fundamental strength of the relationship between soil moisture and fire activity at long lead-times and are indicative of that relationship's utility for the future development of national-scale predictive capability.

61
62
63
64
65
66
67
68
69
70
71
72
73
74
75
76
77
78
79
80
81

1. INTRODUCTION

Wildfires in the United States have increasingly become larger and more frequent during the last several decades, contributing to greater environmental degradation, property damage, and economic losses (Dennison et al. 2014, Morton et al. 2003). By 2025, the cost of fire suppression in the United States is predicted to increase to nearly \$1.8 billion per year (United States Department of Agriculture Forest Service 2015). As a result, there is growing need for the capability to direct operational fire resources before the fire season begins. This points to the growing importance of seasonal to sub-seasonal forecasting capacity for wildfires, similar to those that are being developed for weather and natural resources management (National Academies of Sciences, 2016).

Wildfires are typically defined as uncontrolled fires that occur in areas of combustible vegetation, and depend greatly on vegetation type, structure, arrangement, and moisture. In the contiguous United States, 90% of wildfire ignitions are associated with human activity, but several other environmental factors such as fuel availability, fuel moisture, wind, and lightning strikes can be of critical importance in ignition and growth. The largest contributing factors to general wildfire risk are the pre-fire-season accumulation of fuels and changing fuel moisture content (FMC), both of which can contribute to greater fire severity in a given region. Depending on the vegetation class, more fuels and lower FMC generally indicate higher fire risk and greater fire severity potential—the degree of environmental change caused by a fire (e.g. Verbesselt et al. 2002; Van Der Werf et al. 2008).

1
2
3 82 The spatial distribution and the moisture content of transient (i.e. fast-growing) fuels tend to be
4 83 associated with precipitation and soil moisture conditions at the land surface over the months prior
5 84 to fire season, when some regions experience an annual wet period or rainy season (Chuvieco et
6 85 al. 2004; Krueger et al. 2015). These results suggest that soil moisture may be a good predictor of
7 86 fire occurrence and fire severity, even at seasonal lead times.
8
9 87

10
11 88 However, in order to understand this relationship, the required local-scale that are adequately
12 89 discretized and have a spatially and temporally uniform structure are difficult to obtain over large
13 90 domains (Famiglietti et al. 2008). Therefore it is challenging to develop a quantitative description
14 91 of the relationship between land surface wetness conditions in the period before fire-season and
15 92 wildfire occurrence during the fire season, and the specific impacts of surface moisture conditions
16 93 on wildfire occurrence across land cover types is largely unquantified.
17
18 94

19
20 95 The National Interagency Fire Center currently publishes seasonal fire potential outlook reports
21 96 for the United States (Predictive Services, National Interagency Fire Center 2016). These reports
22 97 use the US Drought Monitor, past monthly temperature and precipitation deviations from average,
23 98 and one and three-month weather outlooks to qualitatively assess regional fire potential. The fire
24 99 potential maps produced offer a tercile assessment—normal, above normal, or below normal—of
25 100 fire potential over broad geographic regions. This method does not currently apply a numerical
26 101 relationship between seasonal fire occurrence and variability in contributing environmental factors
27 102 such as soil moisture. It also does not yet produce a quantitative estimate of probable fire
28 103 occurrence that could be used in a risk-assessment framework.
29
30 104

31
32 105 The Palmer Drought Severity Index (PDSI), additionally, has been shown to have utility in
33 106 assessing drought impacts on wildfire activity (Xiao and Zhuang 2007). However, the PDSI,
34 107 similar to the National Interagency Fire Center outlook reports, is based on temperature and
35 108 precipitation sums and not actual soil moisture observations, and has been shown to be biased for
36 109 assessment of drought conditions in some cases (Sheffield et al. 2012). Burgan et al. (1998) also
37 110 developed a fire danger fuel model map across different ecoregions, largely based on satellite
38 111 NDVI observations, but no soil moisture record was then available. These studies provide both a
39 112 precedent and evidential basis for the use of large-scale climatological variables in wildfire
40 113 assessment. The recent availability of large-coverage soil moisture products, specifically those
41 114 produced in a combination of remote sensing and land-surface model simulations through
42 115 numerical data assimilation, now offer the ability to quantify such relationships at finer scales and
43 116 across large-domains. The development of these data sets should provide a unique opportunity for
44 117 advancement in seasonal wildfire risk assessment.
45
46 118

47
48 119 This study thus seeks to integrate NASA earth observation data and the USDA Forest Service's
49 120 historical fire record to quantify climatic relationships with fire activity. Model-assimilated
50 121 hydrology observations are leveraged to examine finer spatial and longer temporal scales and to
51
52
53
54
55
56
57
58
59
60

1
2
3 122 establish the quantitative basis for seasonal forecasting relationships. Since pre-season soil
4 moisture can serve as a proxy for pre-season fuel accumulation and live fuel moisture conditions,
5 a historical record of remotely sensed soil moisture data products was examined to disentangle the
6 bearing pre-fire season soil moisture conditions have on a succeeding year's fire activity. With a
7 proven statistical relationship, the methods developed herein can in turn be applied to improve fire
8 prediction and risk assessment capabilities in the contiguous US. As more communities in the earth
9 sciences work at achieving seasonal to sub-seasonal (S2S) predictive capabilities, the importance
10 to society of knowing what might happen at several months lead-time is clear.
11
12
13
14
15

16 131 Launched in 2002, NASA's Gravity Recovery and Climate Experiment (GRACE) mission
17 provides monthly observations of terrestrial water storage anomalies (TWSA) that describe spatial
18 and temporal changes in the amount of water stored in soils, groundwater and above the land
19 surface (Tapley et al. 2004), which have proven useful in the monitoring of changing hydrologic
20 conditions (e.g. Famiglietti et al. 2011). However, GRACE observations have an intrinsically low
21 spatial resolution ($\sim 150,000 \text{ km}^2$), due to the altitude of the satellites. This makes GRACE TWSA
22 observations difficult to apply for natural resource management. One way to circumvent the
23 resolution limitations of GRACE is to perform a physical downscaling of the GRACE observations
24 through numerical data assimilation. This has been done with much success for drought and flood
25 monitoring applications (Houborg et al. 2012, Reager et al. 2015), and is currently included as an
26 input to the U.S. Drought Monitor framework (Hobourgh et al. 2012). The resulting surface soil
27 moisture data, downscaled from raw GRACE data with the CLSM, form the base climatic
28 independent variable in this study.
29
30
31
32
33
34
35
36
37
38
39
40
41
42
43
44
45
46
47
48
49
50
51
52
53
54
55
56
57
58
59
60

44 144 Building upon these successes, we investigate the relationship between GRACE-assimilated
45 seasonal surface (top several centimeters) soil moisture (Zaitchick et al. 2008) as a proxy for fuel
46 moisture content and yearly wildfire occurrence and burn extent. We apply GRACE-assimilated
47 soil moisture simulations downscaled with the Catchment Land Surface Model (CLSM) and in-
48 situ wildfire observations over the continental United States during the 2003-2012 period (Short
49 2015), at 0.25-degree spatial resolution, with the 2012-2013 data withheld for validation. Each
50 grid cell represents approximately 785.18 km^2 , or 194022.02 acres. While other remotely sensed
51 soil moisture data products exist, such as those derived from Soil Moisture and Ocean Salinity
52 (SMOS) and AMSR-E/Aqua, these GRACE-assimilated data offer monthly datasets over a long
53 temporal record and with higher spatial resolution that are more ideal for calibrating a historical
54 regression model over the contiguous United States. We disaggregate the study domain by land
55 cover type (Homer et al. 2015), under the hypothesis that wetness should modulate different land
56 cover responses to wildfire ignition differently. Surface soil moisture alone, as opposed to root
57 zone moisture content and total terrestrial water storage, was utilized in order to optimally capture
58 seasonal variance in wetness that affects all dominant species across land cover types, including
59 grasses with shallow roots (Famiglietti et al. 1999). Additionally, utilizing surface soil moisture in
60 this way provides a reference model that can then be applied with future Soil Moisture Active
Passive (SMAP) data. We then determine the historic relationship between wildfire occurrence

1
2
3 163 and CLSM-assimilated surface soil moisture across land cover types, and cross-validate a
4 predicted response to show the strength of the relationship. In doing so, this study reveals complex
5 nonlinearities in the influence of fuel moisture content on wildfire severity, and further establishes
6 the need to incorporate accurate surface moisture information in the quantitative assessment of fire
7 risk and potential in the United States. The aim of this study is to demonstrate a relationship
8 between pre-season soil moisture and fire occurrence likelihood and to characterize large-scale
9 fire sensitivity to seasonal moisture patterns.
10
11

12 170
13 171 2. DATA AND MODELS
14 172
15 173 2.1 GRACE AND CLSM-DA
16 174
17 175 NASA's GRACE mission consists of two Earth-observing satellites orbiting in tandem and spaced
18 176 about 220 kilometers apart at roughly 450 km altitude. A K-band Ranging System (KBR) provides
19 177 precise measurements (within 10 μm) of the distance between the satellites caused by spatial and
20 178 temporal fluctuations in the Earth's gravity field (Tapley et al. 2004). These measurements are
21 179 used to determine variations in the Earth's mass distribution at a horizontal resolution of 150,000
22 180 km^2 , with generally higher measurement accuracy across larger spatial scales (Wahr et al. 2004).
23 181 The monthly to decadal temporal changes in the gravity field are attributed primarily to mass
24 182 redistribution in the atmosphere, ocean, continents and solid earth. After isolation and correction
25 183 of 'unwanted' signals for hydrology applications (i.e. ocean, atmosphere, and postglacial rebound),
26 184 these measurements, referred to as terrestrial water storage anomalies (TWSA), are assumed to
27 185 approximate the movement of water mass over time. Swenson and Wahr (2004) and Wahr et al.
28 186 (1998) offer general post-processing logistics and Landerer and Swenson (2012) offer specifics on
29 187 scaling, signal restoration, and regional error calculation. The GRACE dataset utilized for this
30 188 project is processed by the Texas Center for Space Research (CSR; version CSR-RL05) and
31 189 NASA's Jet Propulsion Laboratory. It is a global, monthly, one degree gridded, scaled GRACE
32 190 land data product available for download at grace.jpl.nasa.gov. The data for this project is from
33 191 the time period April 2002 to December 2013.
34
35

36 192
37 193 Developed at the NASA Goddard Space Flight Center, The Catchment Land Surface Model
38 194 (CLSM) is a physically based land surface model (Koster et al. 2000). For the model forcing, the
39 195 horizontal structure of a rectangular atmospheric grid is separated into topographically-defined
40 196 catchments with an estimated average area of 4000 km^2 . Water is spatially and vertically
41 197 distributed in the model determined by topography and the model's hydrologic processes are
42 198 generally determined by the catchment's topographical statistics. In the assimilation algorithm, the
43 199 model-generated terrestrial water storage moisture elements are corrected with the GRACE
44 200 observational estimate using an Ensemble Kalman Smoothing Filter method (EnKS) as described
45 201 in Zaitchik et al. (2008). Assimilation incorporates the relative uncertainty in the model and the
46 202 observations. In this process, a two-step smoother is applied to manage GRACE's monthly
47 203 temporal resolution both forward and backwards in time. In order to create consistency among
48 204
49 205
50 206
51 207
52 208
53 209
54 210
55 211
56 212
57 213
58 214
59 215
60 216

1
2
3 204 observed and modeled variables, the GRACE water storage anomalies are changed to absolute
4 values by adding the simulated time mean water storage variable from the CLSM output to the
5 observations. The observations are directly applied to the column-integrated forecasted variable
6 (the catchment deficit) and the primary non-equilibrium prognostic (the root zone excess
7 moisture), and the vertical disaggregation occurs based on covariance. The CLSM-Data
8 Assimilation (CLSM-DA) data used in this study extend from January 2003 to December 2014,
9 and the outputs are reported on 0.25-degree grid cells for the contiguous United States. The gridded
10 analysis used in this paper is an interpolation of catchment tiles to an equally spaced model grid
11 for consistency with the other data sets used. Resampling these other datasets to the coarser
12 resolution always introduces uncertainty but captures more first order climatic characteristics.
13
14 214
15
16 215 **2.2 FIRE PROGRAM ANALYSIS-FIRE OCCURRENCE DATABASE**
17
18
19 217 The USDA Forest Service's Fire Program Analysis Fire-Occurrence database (FPA FOD) is a
20 comprehensive geospatial database of wildfires in the United States from 1992 to 2013. It includes
21 1.73 million geo-referenced wildfire records, representing a total of 126 million acres burned
22 during the 22-year period (Short 2015). It also contains vital information for each of these fires,
23 including date, cause, fire size, fire class, burned area, and coordinates. These data were imported
24 as points into a geographic information system and processed into two separate raster datasets that
25 matched the spatial and temporal resolution of the GRACE derived soil moisture data. The first
26 dataset aggregated the annual number of fires in each 0.25×0.25 degree cell for May through
27 April of the following year, while the second summed the total burned area (in acres) for each cell
28 in that timeframe.
29
30 227
31
32 228 **2.3 NATIONAL LAND COVER DATABASE**
33
34
35 229 The land cover type dataset used in this study was the USGS' National Land Cover Database 2011
36 (NLCD 2011) (Homer et al. 2015). This dataset maps land cover and land use across the United
37 States at a 30 meter resolution. The NLCD data were first reclassified for generalization and
38 resampled to the same spatial extent and resolution as the previous two datasets using a majority
39 resampling technique that allocates each pixel's class based on the most popular value within a 3
40 by 3 window. This allowed each grid cell to have a unique land cover classifier, which could then
41 be programmatically used to extract values and characterize each relevant vegetation type's
42 relationship between soil moisture and wildfire. For the purposes of this study, only vegetated land
43 cover types are of importance to wildfires. Accordingly, the Developed/Urban, Barren Land, and
44 Planted/Cultivated classes were not considered in the analysis. The Mixed Forest class was not
45 considered due to its unsuitably small number of pixels. Additionally, even though model
46 simulations of wetland soil moisture may not be accurate due to missing physical processes, we
47 include this class to represent general wet/dry responses in wetland environments. Figure 1 shows
48 a visualization of this processed land cover data along with the other two datasets mentioned above.
49
50 244
51
52
53
54
55
56
57
58
59
60

245 3. METHODS

246
247 *3.1 DATA PROCESSING*

248
249 The first step in algorithm development was to disaggregate the fire data by wildfire size class
250 (Table 1). Annual January through April (2003-2014) soil moisture from the GRACE-derived
251 CLSM-DA data were averaged into single two-dimensional maps (latitude × longitude) for each
252 year that depict a fire season's antecedent moisture conditions (Xystrakis et al. 2014). Annual total
253 fire occurrence and cumulative burned area maps, aggregated from the rasterized FPA FOD data,
254 were produced for each wildfire class, covering the period ranging May through April of the
255 following year. This time period was selected in order to delineate a nominal fire season in line
256 with the beginning of the Western US fire season, although true fire season tends to vary in time
257 and by location (Westerling et al. 2003). Within each land cover type, all burned area and fire
258 occurrence values—which here refers to the total number of fires occurring in a given grid cell—
259 were plotted against corresponding CLSM-DA soil moisture values for the entire population of
260 0.25-degree grid cells. While wildfires belonging to a smaller size class constitute only a fraction
261 of a percent of their parent grid cell, the frequency of their occurrence within each discretized area
262 is an important climatological figure linking soil moisture to fire activity.

263
264 This produced a distribution of fire occurrence, visible in Figure 1, and burned area as a function
265 of soil moisture for each land cover class. These data were then binned by soil moisture ranges to
266 calculate average fire occurrence and burned area values over each range. These distributions
267 reveal the unique relationship in each land cover class between occurrence of wildfires of
268 increasing size classification as a function of soil moisture state. These relationships were then
269 individually modeled by fitting an exponential or linear function depending on which resulted in
270 a higher R² value. If neither function's R² surpassed 0.5, meaning pre-season soil moisture explains
271 less than 50% of the variance in fire activity, mean number of fires and mean burned area were
272 plotted instead. This methodology is displayed for fire occurrence in Figure 2 for each land cover
273 type and fire size class, and the same method was followed for burned area.

274
275 We also investigated whether the information contained in these relationships with soil moisture
276 demonstrated predictive utility. Comprehensive deterministic prediction is challenging, because
277 we don't include all of the information required to determine the comprehensive source and forcing
278 for all fire occurrence and severity; variables such as lightning strikes, human activity, wind gusts,
279 and fuel loading all contribute substantially to actual wildfire predictability. Instead, we investigate
280 a statistical tendency of soil moisture to affect wildfire occurrence by lumping a large population
281 of observations into a single model, and evaluating how the population responds as whole to this
282 single factor. We assume that the population captures the probable best estimate of the relationship
283 that would occur at a single location under different conditions and across time. A comprehensive
284 fire prediction model could likely include other forcing variables.

285

58

59

60

1
2
3 286 *3.2 PREDICTIVE MODEL*
4
5 287

6 288 Each modeled distribution's fitted function or mean was referenced for mapping fire probability
7 289 and predicted burned area. Fire probability and average burned area were calculated by applying
8 290 each individual pre-season soil moisture value to the function corresponding to its land cover type
9 291 for the relevant fire size class. Probable total burned area (Equation 1) is then estimated by
10 292 multiplying the modeled fire occurrence by the modeled average burned area value for each cell's
11 293 soil moisture value as broken down by land cover type and fire size class.
12
13 294
14
15 295 Probable Burned Area(i) = Fire Occurrence(SM_i, LC_i) \times Average Burned Area(SM_i, LC_i)
16
17 (1)
18
19 296
20 297
21 298 In Equation 1, i is a given 0.25 degree grid cell, and SM_i and LC_i are the corresponding values of
22 299 soil moisture and land cover classification. Maps for both predicted number of fires and predicted
300 301 burned area were thus created for each fire size class. These maps, binned by fire size for each
302 303 parameter, can be added together to create maps for a year's total predicted number of fires and
304 305 total burned acreage.

26 303
27 304 **4. RESULTS**
28
29 305

30 306 Figure 2 shows that within each land cover type, there are different distributions of fire occurrence
31 307 as a function of soil moisture for each fire class. For example, within the evergreen forest type, the
32 308 smaller fire classes B, C, and D tend to be more frequently associated with a higher average number
33 309 of fires following high pre-fire season soil moisture. Meanwhile, the larger fire classes E, F, and
34 310 G, show the opposite trend whereby dryer soil moisture conditions in January – April are
35 311 associated with more fires throughout the following year. Some distributions are relatively uniform
36 312 and showing little variability. This indicates the absence of a clear relationship between soil
37 313 moisture and fire occurrence, or that other factors tend to mask that relationship. Each vegetation
38 314 type differs from the other in its surface soil moisture and fire occurrence and size patterns.
39 315 Deciduous forest tends to be the wettest modeled ecosystem (mean volumetric water content
40 316 fraction = 0.31, standard deviation = 0.06) and shrubland tends to be the driest (mean volumetric
41 317 water content fraction = 0.19, standard deviation = 0.05). Wetland ecosystems have the most fires
42 318 per cell on average (11.46 fires per year, standard deviation = 16.79), while shrublands have the
43 319 fewest (3.48 fires per year, standard deviation = 9.16). These values were calculated by compiling
44 320 the preseasong surface soil moisture and fire occurrence values across all cells within each land
45 321 cover type for each year in the study period. These values indicate the need to disaggregate the
46 322 relationship between fire occurrence and soil moisture by land cover type, as each type shows a
47 323 significantly different fire response to soil moisture levels.
48
49 324
50
51
52
53
54
55
56
57
58
59
60

Figure 3 provides an example of results by hindcasting the May 2012 – April 2013 fire year. The top map shows the total number of fires expected to occur in each cell that year based on the

1
2
3 327 preceding January – April average soil moisture. Figure 3 (bottom) shows total predicted burned
4 acreage. The spatial gaps in the predictive maps represent the withheld land cover classes. These
5 maps were created for each year in the study period, and their summary statistics for predicted
6 number of fires and total burned acres were compiled and charted in Table 2 and Figure 4.
7
8 331
9
10 332 To validate these results, predicted fire occurrence and burned area maps that were generated for
11 the 2012 – 2013 fire year (i.e. the most recent year in the FPA FOD dataset), and compared against
12 the observations. For proper cross-validation, this fire year was held out of the algorithmic step.
13 Results are compiled in Table 2. Additionally, the processed FPA FOD data was disaggregated by
14 land cover type and charted next to the predicted fire data, as shown for May 2012 – April 2013
15 in Figure 4, showing the relative accuracy of the algorithm’s prediction for each vegetation type
16 with standard percent error calculations (Equation 2).
17
18 338
19
20 339

$$\%_{error} = \left| \frac{\#_{experimental} - \#_{theoretical}}{\#_{theoretical}} \right| \times 100 \quad (2)$$

21
22 340 Vegetation types that were deemed unsuitable for the analysis (i.e. mixed forest, agricultural, and
23 urban) were removed from the data sets. Figure 4 shows that in the 2012 – 2013 case study, the
24 values for predicted fire occurrence and burned area match the actual data within an error of
25 13.89% and 9.52% respectively, compared to an average error 13.10% for predicted fires and
26 119.40% for predicted burned area for the entire study period.
27
28 341
29
30 342
31
32 343
33
34 344
35
36 345
37
38 346
39
40 347
41
42 348 5. DISCUSSION AND CONCLUSIONS
43
44
45
46
47
48
49
50
51
52
53
54
55
56
57
58
59
60

349 It should be noted that the predictive maps presented are not intended to offer an accurate hindcast
350 of actual fire occurrence and severity in individual 0.25-degree grid cells. Rather, they offer an
351 assessment of the relationship between seasonal soil moisture and wildfire potential, specifically
352 the sensitivity of fires in the fire season to pre-season surface moisture conditions. The modeled
353 functions and validation results show that the total number of fires and burned area predicted is in
354 fact correlated with the pre-season soil moisture data for the corresponding year, across the land
355 cover grouping. A positive correlation would indicate that high pre-season soil moisture is
356 followed by high fire activity, while a negative correlation would see low fire activity. Regional
357 hindcasting of fire occurrence was performed by aggregating the land-cover consistent regions in
358 their entirety over the contiguous US, and optimizing the fire response model for each land cover
359 type. This improves upon an ecoregion approach for which a number of included land cover types
360 may exist, and a corresponding number of fire responses to moisture may occur (e.g. Parks et al.
361 2014). The strong correlation achieved in our results highlights the principal importance of
362 preseason soil moisture in governing fire risk and potential, likely as a proxy for preseason fuel
363 accumulation.
364
365

1
2
3 366 These results provide the first evidence that pre-season soil moisture and wildfire occurrence can
4 be strongly negatively correlated across land cover types. In all land covers, the smaller fire classes
5 (i.e. class “D” or smaller, <300 acres) are generally (11 out of 20 scenarios) associated with higher
6 pre-season soil moisture, not lower soil moisture as hypothesized. This likely describes a situation
7 in which smaller and quick-growing vegetation (e.g. grasses and understory) are more prolific in
8 wet years, and tend to contribute to wildfire persistence and propagation after ignition. As the
9 resampled NLCD 2011 data was implemented in our algorithm, land cover is assumed to be static
10 over the study period. It is possible that this represents an additional error source in our regression,
11 though there is no clear pattern in the percent error figures (Table 2) and land cover changes may
12 represent a small fraction of the regressed relationships across the entire aggregated domain. The
13 random error structure suggests that the model error is more associated with year-to-year weather
14 and soil moisture patterns rather than land-cover change. As soil moisture in this study is used as
15 a proxy for vegetation moisture and general climate conditions, a wet pre-season in certain
16 vegetation types is correlated with more primary production creating increased fuel availability
17 when fire season arrives. This is further corroborated by observations made by Xystrakis et al.
18 (2014), which saw high spring precipitation succeeded by high burned area values. The case that
19 would lead to the most fires in these land cover types is likely that of a very wet pre-season,
20 followed by a very dry fire season. This relationship has been studied before using precipitation
21 observations (e.g. Holden et al. 2007).
22
23 385
24
25 386 While the necessity is clear, the feasibility of wildfire predictive capabilities is increasing with the
26 advent of innovative applications of new remote sensing data. As our analysis focused on
27 quantifying and validating the overall relationship between pre-season soil moisture and
28 succeeding fire activity rather than providing accurate annual fire activity predictions, model
29 outputs are not intended to be applied as accurate annual fire activity predictions. While the model
30 illuminates this relationship, its performance may be negatively affected by limitations in the
31 datasets and omitted environmental factors. For one, resampling the NLCD land cover to the
32 coarser GRACE-DA resolution inevitably decreased the purity of each pixel’s designated land
33 cover type. Using finer-scale SMAP data to expand this analysis may mitigate these effects, and
34 additionally improve the retrieval of burned area. Since accurate, observation-based surface soil
35 moisture information has been difficult to obtain over large domains, GRACE-assimilated model
36 outputs may offer a unique contribution to fire severity prediction methods. This builds upon
37 successes in using GRACE-assimilated model outputs for hydrologic drought monitoring
38 (Houborg et al. 2012), and reinforces the importance of the relationship between large-scale
39 hydrologic forcing and fire response. The current NASA SMAP mission (Entekhabi et al. 2010),
40 launched January, 2015, offers global observations of radiometer-based surface soil moisture at a
41 base 36-km spatial resolution that can be used in conjunction with GRACE-assimilation efforts
42 and should generally improve this methodology. The expanding temporal and spatial coverage of
43 soil moisture brought about by SMAP will additionally allow this methodology to be applied in
44 regions with more heterogeneous land cover conditions due to higher resolutions. These more
45 complex regions may also be approached with regionally sensitive environmental parameters to
46
47 385
48
49 386 While the necessity is clear, the feasibility of wildfire predictive capabilities is increasing with the
50 advent of innovative applications of new remote sensing data. As our analysis focused on
51 quantifying and validating the overall relationship between pre-season soil moisture and
52 succeeding fire activity rather than providing accurate annual fire activity predictions, model
53 outputs are not intended to be applied as accurate annual fire activity predictions. While the model
54 illuminates this relationship, its performance may be negatively affected by limitations in the
55 datasets and omitted environmental factors. For one, resampling the NLCD land cover to the
56 coarser GRACE-DA resolution inevitably decreased the purity of each pixel’s designated land
57 cover type. Using finer-scale SMAP data to expand this analysis may mitigate these effects, and
58 additionally improve the retrieval of burned area. Since accurate, observation-based surface soil
59 moisture information has been difficult to obtain over large domains, GRACE-assimilated model
60 outputs may offer a unique contribution to fire severity prediction methods. This builds upon
successes in using GRACE-assimilated model outputs for hydrologic drought monitoring
(Houborg et al. 2012), and reinforces the importance of the relationship between large-scale
hydrologic forcing and fire response. The current NASA SMAP mission (Entekhabi et al. 2010),
launched January, 2015, offers global observations of radiometer-based surface soil moisture at a
base 36-km spatial resolution that can be used in conjunction with GRACE-assimilation efforts
and should generally improve this methodology. The expanding temporal and spatial coverage of
soil moisture brought about by SMAP will additionally allow this methodology to be applied in
regions with more heterogeneous land cover conditions due to higher resolutions. These more
complex regions may also be approached with regionally sensitive environmental parameters to

1
2
3 407 generate more accurate regional predictive fire maps. For example, the classification of large
4 408 swaths of Minnesota and Michigan as wetland in the NLCD (Figure 1) caused those areas' fire
5 409 frequency to be greatly overestimated as a result of the high fire activity in Florida's Everglades
6 410 and other wetland regions (Figure 3). Indeed, the wetland regression models (Figure 2) do not
7 411 show high correlation coefficients except in the case of large fires, indicating regional processes
8 412 controlling the majority of the variance. Other regional drivers of fire activity that see great spatial
9 413 and temporal variability, such as fuel moisture, wind, and lightning patterns may (Veraverbeke et
10 414 al. 2017) may further reduce the modeled discrepancies in fire occurrence and intensity. Along
11 415 with the finer-scale SMAP data, the fundamental relationship between soil-moisture and fire
12 416 activity observed in this study could be built upon using other environmental variables to generate
13 417 monthly regional predictive fire maps.
14
15
16
17
18
19
20
21
22
23
24
25
26
27
28
29
30
31
32
33
34
35
36
37
38
39
40
41
42
43
44
45
46
47
48
49
50
51
52
53
54
55
56
57
58
59
60

6. ACKNOWLEDGMENTS

This research was conducted at the Jet Propulsion Laboratory, California Institute of Technology, under contract with NASA. We would like to thank Mark Finney and Chuck McHugh, from the USDA Forest Service Predictive Services Program for their involvement in providing direction and information pertaining to wildfires in the United States. This work was supported by the NASA DEVELOP program, through contract NNL11AA00B and cooperative agreement NNX14AB60A. Funding sources include the NASA Applied Sciences Program and the NASA GRACE Science Team. The data supporting this study's conclusions consist of the included tables and figures. The FPA FOD data (*Short, 2015*) can be accessed at <http://dx.doi.org/10.2737/RDS-2013-0009.3>. The assimilated GRACE data is available at <http://grace.jpl.nasa.gov>. The NLCD 2011 is available at <http://www.mrlc.gov/nlcd2011.php>.

7. REFERENCES

- Burgan, R., Klaver, R., & Klaver, J. (1998). Fuel Models and Fire Potential From Satellite and Surface Observations. *International Journal of Wildland Fire*, 8(3), 159. <https://doi.org/10.1071/WF9980159>
- Chuvieco, E., I. Aguado, and A. P. Dimitrakopoulos (2004), Conversion of fuel moisture content values to ignition potential for integrated fire danger assessment, *Can. J. For. Res.*, 34(11), 2284–2293, doi:10.1139/x04-101.
- Dennison, P. E., S. C. Brewer, J. D. Arnold, and M. A. Moritz (2014), Large wildfire trends in the western United States, 1984–2011, *Geophys. Res. Lett.*, 41, 2928–2933, doi:10.1002/2013GL058954.
- Entekhabi, D. et al. (2010), The soil moisture active passive (SMAP) mission, *Proc. IEEE*, 98(5), 704–716, doi:10.1109/JPROC.2010.2043918.
- Famiglietti, J., J. Devereaux, C. Laymon, T. Tsegaye, P. Houser, T. Jackson, S. Graham, M. Rodell, and P. van Oevelen (1999), Ground-based investigation of soil moisture variability within remote sensing footprints during the Southern Great Plains 1997(SGP97) Hydrology Experiment, *Water Resources Research*, 35(6), 1839–1851.
- Famiglietti, J. S., Ryu, D., Berg, A. A., Rodell, M., & Jackson, T. J. (2008). Field observations of

- 1
2
3 450 soil moisture variability across scales. *Water Resources Research*, 44(1).
4 451 <http://doi.org/10.1029/2006WR005804>
- 5 452 Homer, C.G., J.A. Dewitz, L. Yang, S. Jin, P. Danielson, G. Xian, J. Coulston, N.D. Herold, J.D.
6 453 Wickham, and K. Megown (2015), Completion of the 2011 National Land Cover Database
7 454 for the conterminous United States-Representing a decade of land cover change
8 455 information. *Photogrammetric Engineering and Remote Sensing* 81(5), 345-354.
- 9
10 456 Houborg, R., M. Rodell, B. Li, R. Reichle, and B. F. Zaitchik (2012), Drought indicators based
11 457 on model-assimilated Gravity Recovery and Climate Experiment (GRACE) terrestrial water
12 458 storage observations, *Water Resour. Res.*, 48(July), doi:10.1029/2011WR011291.
- 13
14 459 Koster, R. D., M. J. Suarez, A. Ducharme, M. Stieglitz, and P. Kumar (2000), A catchment-based
15 460 approach to modeling land surface processes in a general circulation model: 1. Model
16 461 structure, *J. Geophys. Res.*, 105(D20), 24809–24822.
- 17
18 462 Krueger, E. S., T. E. Ochsner, D. M. Engle, J. D. Carlson, D. Twidwell, and S. D. Fuhlendorf
19 463 (2015), Soil Moisture Affects Growing-Season Wildfire Size in the Southern Great Plains,
20 464 Soil Sci. Soc. Am. J., 79(6), 1567–1576, doi:10.2136/sssaj2015.01.0041.
- 21
22 465 Landerer, F. W., and S. C. Swenson (2012), Accuracy of scaled GRACE terrestrial water storage
23 466 estimates, *Water Resour. Res.*, 48(4), 1–11, doi:10.1029/2011WR011453.
- 24
25 467 Morton, D. C., M. E. Roessing, A. E. Camp, and M. L. Tyrrell (2003), *Assessing the
26 468 Environmental, Social, and Economic Impacts of Wildfire*, New Haven, CT.
- 27
28 469 National Academies of Sciences, Engineering, and Medicine (2016) *Next Generation Earth
29 470 System Prediction: Strategies for Subseasonal to Seasonal Forecasts*. Washington, DC: The
30 471 National Academies Press. doi:<https://doi.org/10.17226/21873>.
- 31
32 472 National Significant Wildland Fire Potential Outlook. (2016). Predictive Services, National
33 473 Interagency Fire Center. Boise, Idaho. Retrieved from
34 474 <http://www.predictiveservices.nifc.gov/outlooks/outlooks.htm>
- 35
36 475 Reager, J., Thomas, A., Sproles, E., Rodell, M., Beaudoin, H., Li, B., & Famiglietti, J. (2015).
37 476 Assimilation of GRACE Terrestrial Water Storage Observations into a Land Surface Model
38 477 for the Assessment of Regional Flood Potential. *Remote Sensing*, 7(11), 14663–14679.
39 478 <http://doi.org/10.3390/rs71114663>
- 40
41 479 Rodell, M. (2013), "Application of satellite gravimetry for water resource vulnerability
42 480 assessment", chapter in *Climate Vulnerability: Understanding and Addressing Threats to
43 481 Essential Resources*, Elsevier Inc., Academic press, pp. 151-159.
- 44
45 482 Short, Karen C. (2015). Spatial wildfire occurrence data for the United States, 1992-2013
46 483 (FPA_FOD_20150323). 3rd Edition. Fort Collins, CO: Forest Service Research Data
47 484 Archive. <http://dx.doi.org/10.2737/RDS-2013-0009.3>.
- 48
49 485 Swenson, S., and J. Wahr (2006), Post-processing removal of correlated errors in GRACE data,
50 486 *Geophys. Res. Lett.*, 33(8), doi:10.1029/2005GL025285.
- 51
52 487 Tapley, B. D., S. Bettadpur, J. C. Ries, P. F. Thompson, and M. M. Watkins (2004), GRACE
53 488 measurements of mass variability in the Earth system., *Science* (80-.), 305, 503–505,
54 489 doi:10.1126/science.1099192.
- 55
56 490 The Rising Cost of Fire Operations: Effects on the Forest Service's Non-Fire Work. (2015).
57 491 United States Department of Agriculture Forest Service. Retrieved from
58 492 <http://www.fs.fed.us/sites/default/files/media/2014/34/nr-firecostimpact-082014.pdf>
- 59
60 493 Van Der Werf, G. R., J. T. Randerson, L. Giglio, N. Gobron, and a. J. Dolman (2008), Climate
59 494 controls on the variability of fires in the tropics and subtropics, *Global Biogeochem. Cycles*,
60 495 22, 1–13, doi:10.1029/2007GB003122.

- 1
2
3 496 Veraverbeke, S., B. M. Rogers, M. L. Goulden, R. R. Jandt, C. E. Miller, E. B. Wiggins, and J.
4 497 T. Randerson. 2017. Lightning as a Major Driver of Recent Large Fire Years in North
5 498 American Boreal Forests. *Nature Climate Change* 7 (7): 529–34.
6 499 doi:10.1038/nclimate3329.
7
8 500 Verbesselt, J., S. Fleck, and P. Coppin (2002), Estimation of fuel moisture content towards fire
9 501 risk assessment: a review, in *Proceedings of the 6th International Conference on Forest*
10 502 *Fire Research*.
11
12 503 Wahr, J., M. Molenaar, and F. Bryan (1998), Time variability of the Earth's gravity field:
13 504 Hydrological and oceanic effects and their possible detection using GRACE, *J. Geophys.*
14 505 *Res.*, 103(B12), 205–229.
15
16 506 Wahr, J., S. Swenson, V. Zlotnicki, and I. Velicogna (2004), Time-variable gravity from
17 507 GRACE: First results, *Geophys. Res. Lett.*, 31(11), doi:10.1029/2004GL019779.
18
19 508 Westerling, A. L., A. Gershunov, T. J. Brown, D. R. Cayan, and M. D. Dettinger (2003), Climate
509 and wildfire in the western United States, *Bull. Am. Meteorol. Soc.*, 84(5), 595–604,
20 510 doi:10.1175/BAMS-84-5-595.
21
22 511 Xiao, J. F., & Zhuang, Q. L. (2007). Drought effects on large fire activity in Canadian and
23 512 Alaskan forests. *Environmental Research Letters*, 2(4), 44003. <https://doi.org/Artn 044003\rDoi 10.1088/1748-9326/2/4/044003>
24
25 513 Xystrakis, F., Kallimanis, A. S., Dimopoulos, P., Halley, J. M., & Koutsias, N. (2014).
26 514 Precipitation dominates fire occurrence in Greece (1900-2010): Its dual role in fuel build-up
27 515 and dryness. *Natural Hazards and Earth System Sciences*, 14(1), 21–32.
28 516 <https://doi.org/10.5194/nhess-14-21-2014>
29
30 517 Zaitchik, B. F., M. Rodell, and R. H. Reichle (2008), Assimilation of GRACE Terrestrial Water
31 518 Storage Data into a Land Surface Model: Results for the Mississippi River Basin, *J.*
32 519 *Hydrometeorol.*, 9, 535–548, doi:10.1175/2007JHM951.1.
33
34
35
36
37
38
39
40
41
42
43
44
45
46
47
48
49
50
51
52
53
54
55
56
57
58
59
60

521 8. TABLES

522

523 **Table 1.** Fire Size Class Definitions¹

Class	Burned Acres
A	0 – 0.25
B	0.26 – 9.9
C	10 – 99.9
D	100 – 299
E	300 – 999
F	1000 – 4999
G	5000 +

524 ¹Class size ranges are defined by (Short 2015)

525

526

527 **Table 2.** Predicted and Actual Fire Data with Associated Prediction Errors

	Predicted Fires	Actual Fires	Predicted Burned Acres	Actual Burned Acres	Predicted Fires Percent Error	Predicted Burned Area Percent Error
5/2003 - 4/2004	59410	53542	7356289.94	3333260.32	10.96	120.69
5/2004 - 4/2005	58131	44304	7429770.21	1288883.79	31.21	476.45
5/2005 - 4/2006	61526	72461	7472239.08	6710199.52	11.36	15.09
5/2006 - 4/2007	56998	66903	7343697.15	7181219.66	2.26	14.81
5/2007 - 4/2008	57954	62238	7427601.87	8680825.32	6.88	14.44
5/2008 - 4/2009	56177	59937	7357446.45	3887901.30	6.27	89.24
5/2009 - 4/2010	56337	43507	7407664.38	1603893.48	29.49	361.86
5/2010 - 4/2011	61071	55468	7510430.96	4935915.82	10.10	52.16
5/2011 - 4/2012	57448	52897	7423439.20	5312742.66	8.60	39.73
5/2012 - 4/2013	55442	48679	7559133.21	8354888.73	13.89	9.52

528

529

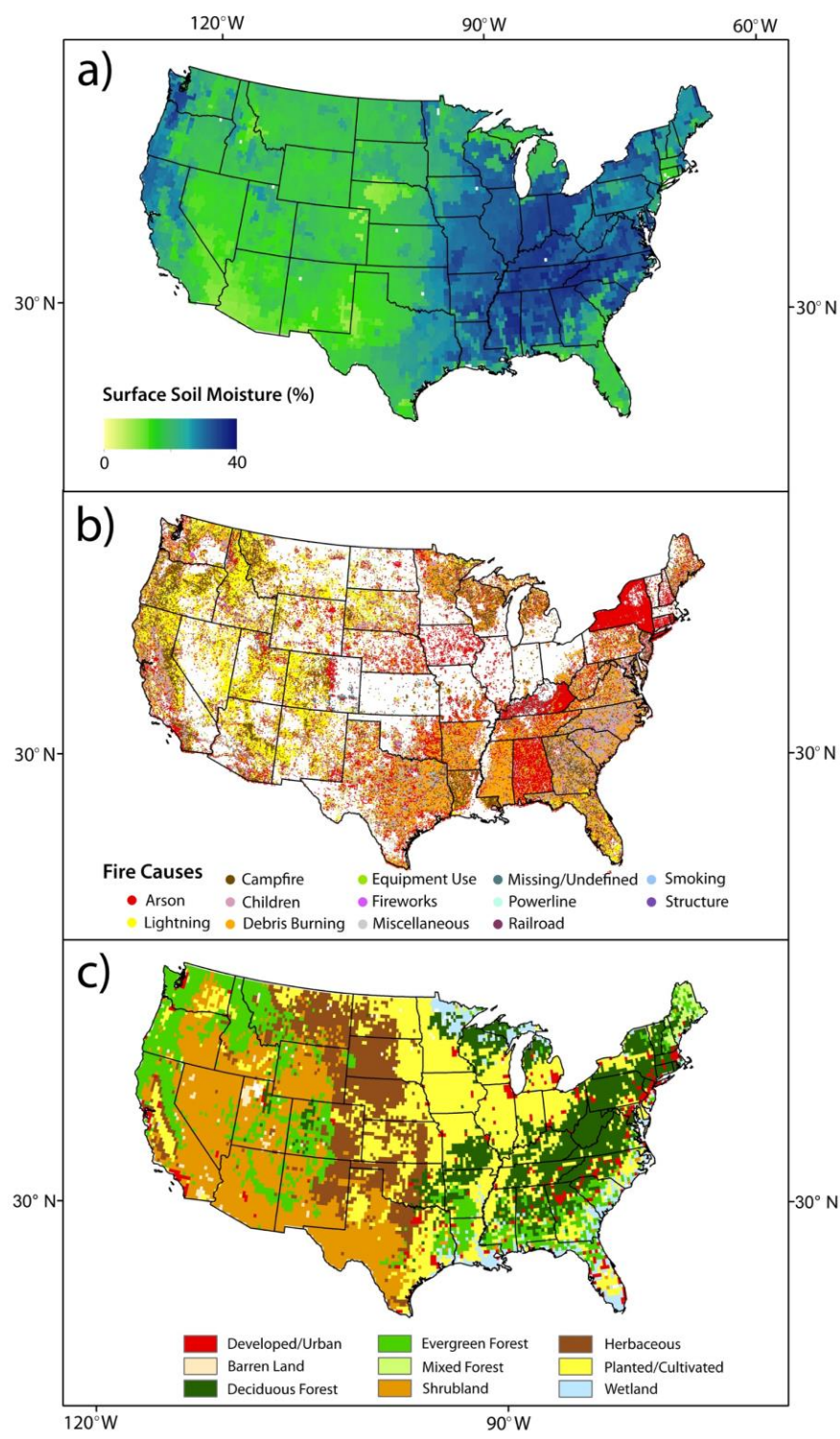
530

531

532

533

534 9. FIGURES



535
536 **Figure 1.** The datasets used in this study: (a) GRACE-derived volumetric surface soil moisture
537 expressed as percent. This example shows average January – April surface soil moisture from 2003
538 – 2013. (b) All fires from the 2003 – 2013 study period in the FPA FOD mapped as points by fire
539 cause. (c) The NLCD 2011 resampled to a 0.25-degree resolution.

540

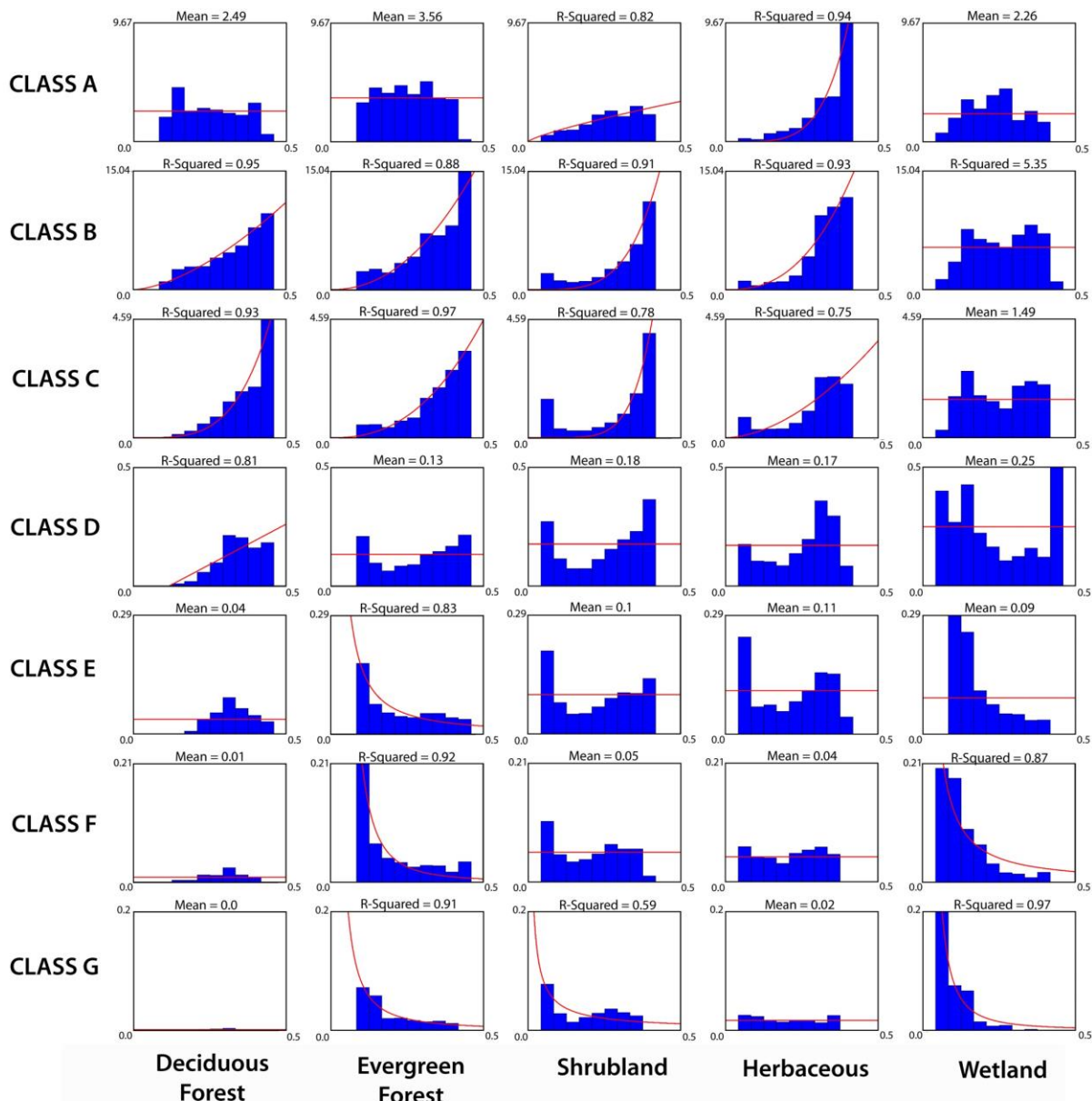
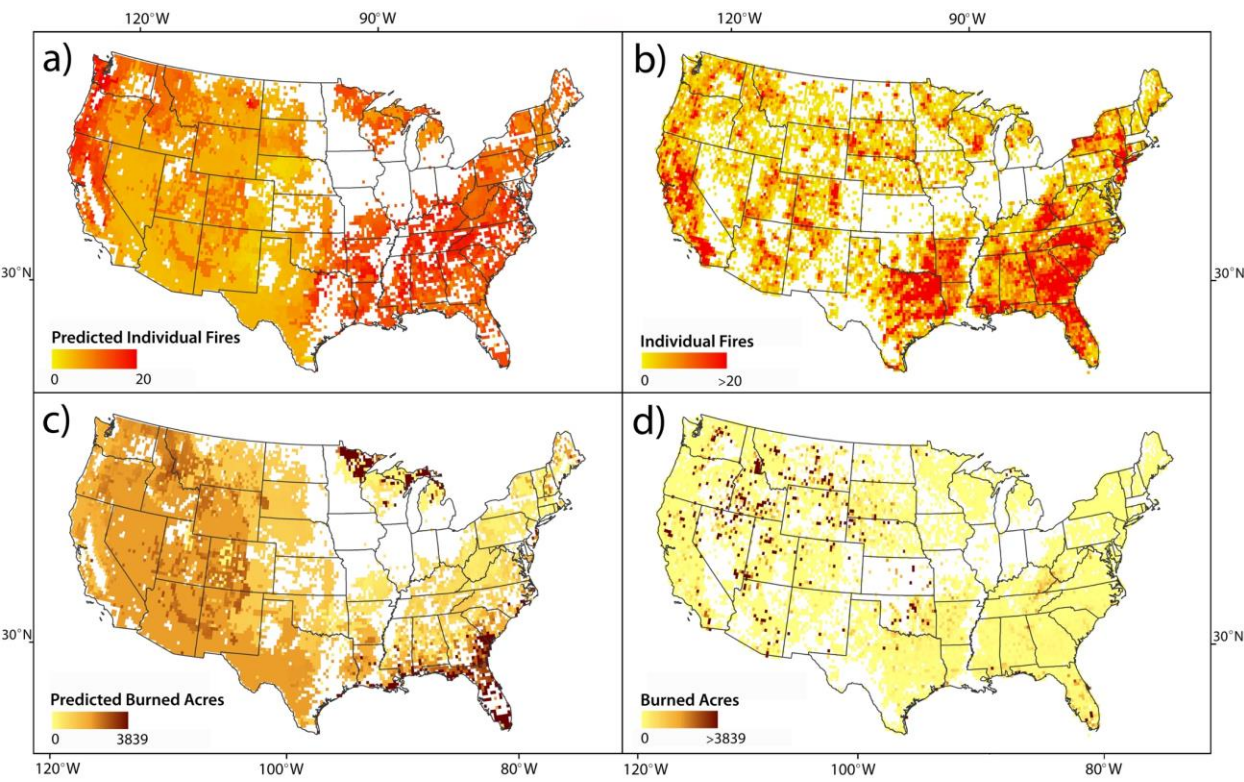
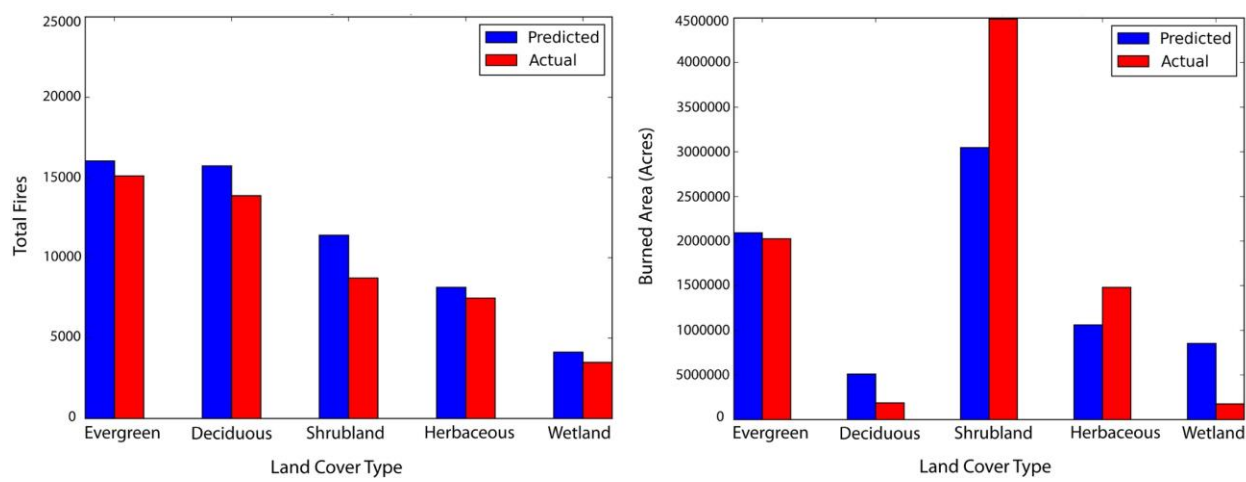


Figure 2. Binned average fire occurrence over each complete year and associated fitted functions or mean values for each analyzed land cover type by fire size class. The x-axis of each chart denotes surface soil moisture as a percentage, and the y-axis shows the average number of fires per 0.25 degree cell for that soil moisture bin. The fire size classes are defined by Short (2015), displayed in Table 1.



549
550 **Figure 3.** Predictive maps for (a) individual fires and (c) burned area to assess fire risk and
551 potential from May 2012 – April 2013. These predictive results are compared against the (b) actual
552 fire distribution and (d) actual burned area for that year for validation.
553

554



555

556 **Figure 4.** Validation of total predicted fires and burned acres from May 2012 – April 2013.